A NOVEL SOLAR-FUEL ASSISTED THERMOPHOTOVOLTAIC SYSTEM AND PARAMETRICAL ANALYSIS

by

Shiquan SHAN[a], Siqi JIA[a], Fan ZHANG[a], Xinyue HAO[b*], Chunhui SHOU[c*], and Zhijun ZHOU[a]

[a] State Key Laboratory of Clean Energy Utilization, Zhejiang University, Hangzhou, China
[b] Ningbo Institute of Technology, Zhejiang University, Ningbo, China
[c] Key Laboratory of Solar Energy Utilization and Energy Saving Technology of Zhejiang Province, Zhejiang Energy Group R&D Institute Co., Ltd, Hangzhou, China

Original scientific paper
https://doi.org/10.2298/TSCI220910192S

In this study, a thermal-balance model is established for energy calculation of a new solar-fuel assisted thermophotovoltaic system, which could save fossil fuels and improve the grade of solar energy. The coupling effects of key parameters such as concentrate ratio, absorber area, emitter area, etc. on the system efficiency are determined. Besides, the effect of solar energy on the fuel saving is investigated. The results show that the solar-fuel assisted thermophotovoltaic system cannot only increase the output power of photovoltaic cells by nearly 25 kW/m^2 compared to fuel-driven thermophotovoltaic but also increase the electrical efficiency by nearly 10 percentage points. Furthermore, it also saves fuel by up to 76%. It is pointed out that improving the absorptance of solar absorber is the key for system optimization. This study provides a reference for the design and application of solar thermophotovoltaic technology.

Key words: *solar energy, thermo-photovoltaic, solar-fuel assisted, parametrical analysis*

Introduction

The development and recovery of the world economy under the epidemic environment have created a large demand for fossil fuels [1], and the consumption of fossil energy has also caused great challenge to environmental protection. In order to achieve the goal of carbon neutrality, on the one hand, it is necessary to develop and utilize renewable resources such as solar energy [2]. Considering the supply discontinuity of solar energy, the use of solar energy and fossil fuel for complementary energy supply is also a key measure to achieve stable utilization of solar energy and save fossil energy under the current technology state. On the other hand, the development of new energy conversion technologies has greater potential in energy efficiency, which is conducive to the development and utilization of renewable energy.

Thermophotovoltaic (TPV), a potential new power generation technology, could convert the thermal energy generated by solar radiation or fuel combustion into radiative energy with adjusted spectrum, which further generate electrical energy through photovoltaic. The TPV also has many advantages such as low noise, light weight, high energy density, and flexible fuel adaptability [3]. A typical TPV system consists of a heat source, emitter, filter, and PV

* Corresponding authors, e-mail: xinyuehao@zju.edu.cn, shouchunhui@zjenergy.com.cn

cell [4]. Fuel-driven TPV heats the emitter via the thermal energy from combustion chamber, thus the emitter can generate spectral radiation in a suitable waveband for PV cells [5]. If concentrated solar radiation is used as a heat source, solar thermophotovoltaics (STPV) is formed [6]. The theoretical thermodynamic efficiency of STPV can reach 85% [7]. Furthermore, the energy conversion efficiency of more than 50% can be achieved through practical design of selective absorber and emitter [8], showing great application potential.

For STPV system, the selective absorber or emitter based on micro/nanostructured materials plays an important role in the system performance [9], Nam *et al*. [10] designed a planar STPV based on 2-D Ta photonic crystals and series filters, achieving a numerical efficiency of 10% at 1400 K. Ni *et al*. [11] designed a STPV for low solar concentration, besides, a cavity-structured reflector is set in front of the absorber to recycle the infrared photons emitted from the absorber top surface, it presented a simulated efficiency of 17.4% at 50 concentration ratio. The selective absorber and emitter based on tungsten spheres and SiO_2-coated substrates designed by Chen *et al*. [12] can be used to match InGaAsSb PV cells. Through numerical calculations, the total STPV efficiency increases from 10.4-20.3% when the incident solar concentration ratio increases from 1-100. For experimental studies, a system efficiency of 3.2% is obtained using a photonic-crystal emitter by Lenert *et al*. [13]. Ungaro *et al*. [14] constructed STPV devices with nanostructured tungsten as selective absorber/emitter and GaSb cells, and obtained an experimental efficiency of 6.2%. Recently, Bhatt *et al.* [15] used two Si_3N_4 nanolayers with an intermediate W layer to form an emitter to fabricate a planar STPV system matching GaSb cell, it shows a system efficiency of 8.6% at 1670 K. Due to various losses, the highest experimental efficiency of STPV is only 10%. However, the recent experiment by La Potin *et al*. [16] determined that the TPV efficiency can reach 40%, which fully demonstrates the development potential of TPV and STPV in the future.

Moreover, due to the discontinuity of solar energy, STPV system needs to be designed and optimized. Seyf *et al*. [17] proposed to use high temperature silicon as thermal storage medium for STPV. Recently, Chen *et al*. [18, 19] proposed to use conventional molten salt energy storage mode for STPV power generation, and the related solar absorber and emitter are designed to achieve a system efficiency of 29% under medium temperature conditions. From another perspective, the discontinuity of solar energy can be overcome by complementing with fuel. Since the combustion of fossil fuel can generate high temperature, the complementation of solar energy and fossil fuel can effectively improve the quality of solar energy and improve its conversion efficiency. There are many similar studies on thermal power cycle. Rovira *et al*. [20] designed a solar-fuel assisted combined cycle and found that after preheating air and then introducing it into the combustion chamber, not only the fuel consumption can be reduced, but also efficiency of thermal power cycle can be improved. Li *et al*. [21] used solar energy as medium-temperature heat source for steam turbine generator and found that the power generation efficiency can be improved. Therefore, it can be determined that the combination of fuel combustion and solar energy for TPV has a distinct application value. In terms of fuel-driven TPV, Li *et al*. [22] proposed to use porous media as the heat source for micro-combustion TPV and use H_2 as fuel. Bani *et al*. [23] further conducted experiments and numerical simulations for similar devices. In addition, Mustafa *et al*. [24, 25] innovatively used kerosene and vegetable cooking oil blends as fuel to conduct experimental research on TPV power generation. Kang *et al*. [26] used CH_4 as the fuel, and experimentally verified that the use of selective filters could improve the performance of TPV with SiC emitter. Recently, Peng *et al*. [27] demonstrated that H_2/C_3H_8/air premixed combustion can be used for micro-TPV, which can enhance flame stability and heat transfer performance. Based on fuel-driven TPV system, Shan *et al*. [28] pro-

posed an innovative integrated system between oxy-fuel TPV device and a Brayton-Rankine combined cycle, which showed higher system efficiency by 20% than the power cycle with similar parameters. Besides, they further [29] proposed a cascade TPV system based on oxy-fuel combustion, which was found to be effective in improving efficiency through optimization analysis. It can be seen that although much research on STPV and fuel-driven TPV has been done, there is few studies about solar-fuel assisted TPV system. It can be determined that the TPV with the complement of fuel combustion and solar energy has the advantages of increasing air preheating temperature, saving fossil fuel, overcoming solar instability, and improving solar energy conversion efficiency. Thus, it's necessary to conduct relevant research. In addition, it should be noted that most previous studies have used commercial software in the numerical simulation and optimization of TPV device. Moreover, most recent studies focus on individual combustion processes [30, 31] or emitter design [32], with few optimization calculation studies considering the combination of combustion and thermal balance modelling.

Against the previous background, this paper presents a parametric analysis of a novel solar-fuel assisted TPV system. The innovative work is:

– A new solar-fuel assisted TPV device is proposed, which overcomes the disadvantage of solar instability and enhances the potential of low grade solar energy utilization.
– A physical model based on thermal balance is developed for system parametric analysis.
– The synergistic effects of key parameters such as concentration ratio, receiver area and emitter area on TPV efficiency are investigated, and some recommendations for practical application are summarized.

It is found that the addition of solar energy can increase the output power of TPV and improve its electrical efficiency by up to 10 percentage points, besides it can also save up to 76% of fuel. This study also provides a reference for the design and application of solar TPV technology.

System models and methods

Solar-fuel assisted TPV system

Figure 1 shows a simplified schematic diagram of a solar-fuel assisted TPV system. It consists of solar collector, combustion chamber, emitter, filter, TPV cell and cooling system. The air is heated by the concentrate solar radiation through solar absorber in the air preheater before entering the combustion chamber, and then enters the combustion chamber to assist the combustion of fuel oil. The outer wall of the combustion chamber is fitted with an emitter made

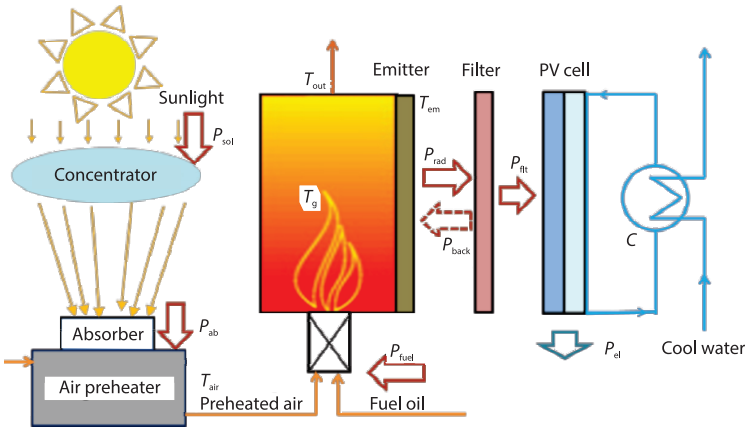

Figure 1. Schematic diagram of solar-fuel assisted TPV system

by SiC material to generate radiative energy P_{rad}, which P_{rad} passes through the filter and releases the short-wavelength radiative energy P_{flt} matching the band gap of the PV cell. Meanwhile, the long-waveband radiative energy P_{back} that does not match the PV cell returns to the combustion chamber. Eventually, P_{flt} reaches the surface of the PV cell. This progress not only elevates the temperature of the emitter, but also helps to increase the output power of the PV cell and improve the system efficiency. Moreover, the PV system is equipped with a circulating cooling system. The cooling water flows over the backside of PV cell and maintains it in an optimal working condition, avoiding the temperature rise of the PV cell [33]. Moreover, the high temperature flue gas from the combustion chamber enters the heat exchanger for further utilization.

Solar collector model

Solar collector generally consists of concentrator and receiver. The concentrated solar radiation is absorbed by solar absorber, which converts the solar energy into heat energy and transmits it to the working fluid. The air preheating process in a solar collector can be defined by eqs. (1)-(3). In this study, only the effect of radiation heat transfer on solar collector is considered since it is the main energy transfer form:

$$P_{ab} = P_{sol}\alpha\rho - S_1\sigma\left(T_a^4 - T_0^4\right) \tag{1}$$

$$P_{ab} = \dot{m}_{air}\left(h_{air} - h_0\right) = \dot{m}_{air}\int_{T_0}^{T_{air}} C_p\left(\text{air}\right)\text{d}T \tag{2}$$

$$P_{sol} = CGS_1 \tag{3}$$

where P_{sol} is the input solar power, P_{ab} [W] – the absorbed power, G – the unit solar radiation, its value is 1000 W/m^2, C – the concentrated ratio, and S_1 [m^2] – the absorber area, and T_{ab}, T_0 [K] are the absorber surface temperature and ambient temperature. The heat transfer coefficient, E_c, between the working fluid and the surface of solar absorber can be expressed:

$$E_c = \frac{T_{air} - T_0}{T_{ab} - T_0} \tag{4}$$

Combustion chamber model

In this study, the fuel input power is set as 10 kW, and the fuel oil could be regarded as *n*-octane (C_8H_{18}), its low level calorific value is 44791 kJ/kg, and the excess air coefficient is taken as 1.1 [28]. The calculation method of the energy-balance model for the whole combustion chamber relies on our previous study [29]. The combustion chamber is simplified as multiple juxtaposed cylinders with a radius of 0.025 m to increase specific surface area. According to the energy balance, as shown in fig. 1, the total energy input to system is the sum of solar energy and the fuel input energy:

$$P_{in} = P_{fuel} + P_{sol} \tag{5}$$

The input energy of the fuel:

$$P_{fuel} = \dot{m}_{fuel}LHV \tag{6}$$

The ratio r of solar energy to fuel input can be expressed:

$$r = \frac{P_{sol}}{P_{fuel}} \tag{7}$$

The adiabatic flame temperature can be expressed by the eq. (8), and the enthalpy of combustion flue gas is defined [34]:

$$\dot{m}_{\mathrm{cp}}\left(h_{\mathrm{af}}-h_0\right)=\dot{m}_{\mathrm{cp}}\int_{T_0}^{T_{\mathrm{af}}}C_p\left(\mathrm{cp}\right)\mathrm{d}t=P_{\mathrm{fuel}}+P_{\mathrm{ab}} \tag{8}$$

The thermal balance between the high temperature flue gas inside the combustion chamber and the emitter radiation is shown below and it is considered that the combustion chamber wall temperature, T_{w}, is approximately the same as the emitter wall temperature, T_{em}:

$$P_{\mathrm{flt}}=\varepsilon_{\mathrm{sys}}\sigma\left(T_{\mathrm{g}}{}^4-T_{\mathrm{w}}{}^4\right)S_2+h\left(T_{\mathrm{g}}-T_{\mathrm{w}}\right)S_2 \tag{9}$$

$$P_{\mathrm{flt}}=\dot{m}_{\mathrm{cp}}\int_{T_{\mathrm{out}}}^{T_{\mathrm{af}}}C_p\left(\mathrm{cp}\right)\mathrm{d}T \tag{10}$$

$$T_{\mathrm{w}}=T_{\mathrm{em}} \tag{11}$$

where h is the convective heat transfer coefficient between flue gas and the wall and is set as 180 W/m^2 K [29].

In addition, the radiative energy passing through the filter can be defined:

$$P_{\mathrm{flt}}=S_2\int_0^{\lambda_{\mathrm{c}}}\varepsilon_{\mathrm{em}}\left(\lambda\right)E_{\mathrm{b}}\left(\lambda,T_{\mathrm{em}}\right)\mathrm{d}\lambda \tag{12}$$

The emissivity, $\varepsilon_{\mathrm{em}}$, is the emitter is set to 0.9 and λ_{c} – the cut-off wavelength of the filter corresponding to the PV cell. In the combustion chamber of this study, the system emissivity is defined:

$$\varepsilon_{\mathrm{sys}}=\frac{1}{\dfrac{1}{\varepsilon_{\mathrm{f}}}+\dfrac{1}{\varepsilon_{\mathrm{w}}}-1} \tag{13}$$

where the emissivity of furnace wall, ε_{w}, is the assumed as 1 and ε_{f} – the flame emissivity is expressed as the weighted sum of the gas emissivity and particle emissivity [35]:

$$\varepsilon_{\mathrm{f}}=m_{\mathrm{u}}\varepsilon_{\mathrm{u}}+\left(1-m_{\mathrm{u}}\right)\varepsilon_{\mathrm{g}} \tag{14}$$

where m_{u} is the ratio of the luminous particles and is set as 0.55 and its emissivity ε_{u} is set as 0.85, ε_{g} is mixed gas emissivity, which is calculated through the weighted-sum-of gray-gases (WSGG) model [36] based on the temperature of the flue gas, the path-length, L, and the molar ratio.

The relationship among average flame temperature, T_{g}, the adiabatic flame temperature, T_{af}, and the outlet flue gas temperature, T_{out}, can be written [37]:

$$T_{\mathrm{g}}{}^4=rT_{\mathrm{out}}{}^4 \tag{15}$$

$$r=\frac{3}{\left(\dfrac{T_{\mathrm{out}}}{T_{\mathrm{af}}}\right)^3+\left(\dfrac{T_{\mathrm{out}}}{T_{\mathrm{af}}}\right)^2+\dfrac{T_{\mathrm{out}}}{T_{\mathrm{af}}}} \tag{16}$$

where the spectral radiation efficiency is defined to evaluate the radiative energy proportion generated by the emitter:

$$\eta_{\text{flt}} = \frac{P_{\text{flt}}}{P_{\text{sol}} + P_{\text{fuel}}} \tag{17}$$

The PV cell

In this study, two PV cells, Si [5] and GaSb [38], with band gaps of 1.1 eV and 0.72 eV are investigated, respectively. Therefore, the cut-off wavelengths of the filter corresponding to these two photovoltaic cells were 1.1 μm and 1.8 μm, respectively.

The output power P_{el} of the photovoltaic cell can be defined [33]:

$$P_{\text{el}} = V_{\text{oc}} \times FF \times J_{\text{sc}} \tag{18}$$

The short-circuit current J_{sc} is calculated:

$$J_{\text{sc}} = \int_{\lambda_0}^{\lambda_c} \frac{q_0 \lambda}{hc} \text{EQE}(\lambda) \varepsilon_{\text{em}}(\lambda) E_b(\lambda, T_{\text{em}}) \text{d}\lambda \tag{19}$$

where EQE is the external quantum efficiency, q_0 – the elementary charge, and h – the Planck constant, and c is the speed of light.

The open circuit voltage can be calculated [29]:

$$V_{\text{oc}} = \frac{\Gamma k T_{\text{c}}}{q_0} \ln\left(\frac{J_{\text{sc}}}{J_0} + 1\right) \tag{20}$$

where k is the Boltzmann constant, Γ – the diode ideality factor, which takes the value of 1 in this study, T_{c} – the surface temperature of the PV cell (constant 300 K), and J_0 – the diode saturation current of the PV cell, which can be calculated using the empirical equation [29]:

$$J_0 = 1.5 \cdot 10^5 \exp\left(\frac{-E_{\text{g}}}{kT_{\text{c}}}\right) \tag{21}$$

The filling factor is calculated using the following equation, and the correction factor β is taken to be 0.96:

$$FF = \beta \frac{v - \ln(v + 0.71)}{v + 1} \tag{22}$$

where v is the normalized open-circuit voltage, which can be defined

$$v = \frac{q_0}{kT_{\text{c}}} V_{\text{oc}} \tag{23}$$

The PV cell efficiency η_{cell} is defined:

$$\eta_{\text{cell}} = \frac{P_{\text{el}}}{P_{\text{flt}}} \tag{24}$$

System efficiency

According to the models, the power generation efficiency of the system is defined as:

$$\eta_{\text{sys}} = \frac{P_{\text{el}}}{P_{\text{sol}} + P_{\text{fuel}}} \tag{25}$$

where in order to investigate the energy-saving effect of the solar-fuel assisted TPV system, the efficiency $\eta_{\text{sys,n}}$ of the TPV system using fuel alone (non-complementary) is specially calculat-

ed. The fuel consumption $P_{\text{fuel,n}}$ of the non-complementary TPV system can be calculated from $\eta_{\text{sys,n}}$ and the electric energy produced P_{el} under specific operating conditions, therefore, the energy saving rate of the solar-fuel assisted TPV system is defined:

$$\theta_{\text{energy}} = \frac{P_{\text{fuel,n}} - \left(P_{\text{sol}} + P_{\text{fuel}}\right)}{P_{\text{fuel,n}}} \tag{26}$$

Moreover, the fuel saving rate of a solar-fuel assisted TPV system is defined:

$$\theta_{\text{fuel}} = \frac{P_{\text{fuel,n}} - P_{\text{fuel}}}{P_{\text{fuel,n}}} \tag{27}$$

where the energy saving effect of the system can be evaluated by θ_{energy} and θ_{fuel}. Based on the aforementioned physical models, the Fortran code is used for programming in this study and the whole simulation flow chart is shown in fig. 2.

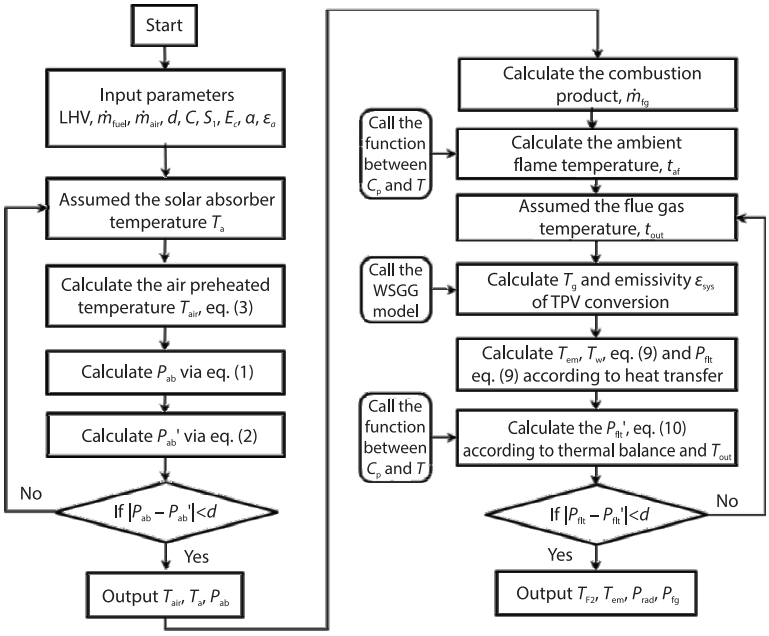

Figure 2. Flow chart of thermal-balance calculation for solar-fuel assisted TPV device

Results and discussion

Effect of different PV cells

In this study, the Si cell and GaSb cell are selected, and the air condition is 21% O_2/N_2. The basic case is set as: the absorptance, α, is 0.9, emittance of absorber ε_a is 0.2, the heat transfer coefficient E_c is 0.8. After the program calculates many cases, three key cases will be selected to analyze the effect of PV cell, which are:

- concentration ratio $C = 400$, receiver area $S_1 = 0.02$ m^2, emitter area $S_2 = 0.3$ m^2,
- concentration ratio C = 500, receiver area $S_1 = 0.025$ m^2, emitter area $S_2 = 0.35$ m^2, and
- concentration ratio $C = 600$, receiver area $S_1 = 0.03$ m^2, emitter area $S_2 = 0.4$ m^2.

As shown in fig. 3, under typical cases, the electrical efficiency of TPV system with Si cell is about 6-8 percentage points higher than that of GaSb cell. This is because the filter for

Si cell has shorter cut-off wavelength. Compared with the GaSb cell, more radiative energy that is not matched with the cell is returned to the combustion chamber by the filter and the P_{flt} is less, which maintains the emitter temperature T_{em}. As shown in fig. 2(b), the emitter temperature using Si cell is always higher than that using GaSb cell (about 380 K) under three cases. Due to the high temperature conditions, the spectrum peak shifts to the short wavelength direction, which makes the cell efficiency of Si cells higher. As shown in fig. 3(d), the efficiency of Si cells is about 13 percentage points higher than that of GaSb cells. Therefore, even under the conditions of low spectral radiative efficiency, fig. 3(c), the electrical efficiency of TPV systems using Si cells is higher than that using GaSb cells. From technical view, Si cells are highly commercialized and can have a design life of about 20 years. It is believed to operate for at least 5 years or more with cooling technology, Since GaSb cells have been produced in small scale, their theoretical life span should be at least 3-5 years. However, the cost of Si cell is much lower than GaSb cell, so it is more suitable for solar-fuel assisted TPV system and the following analysis will focus on Si cell.

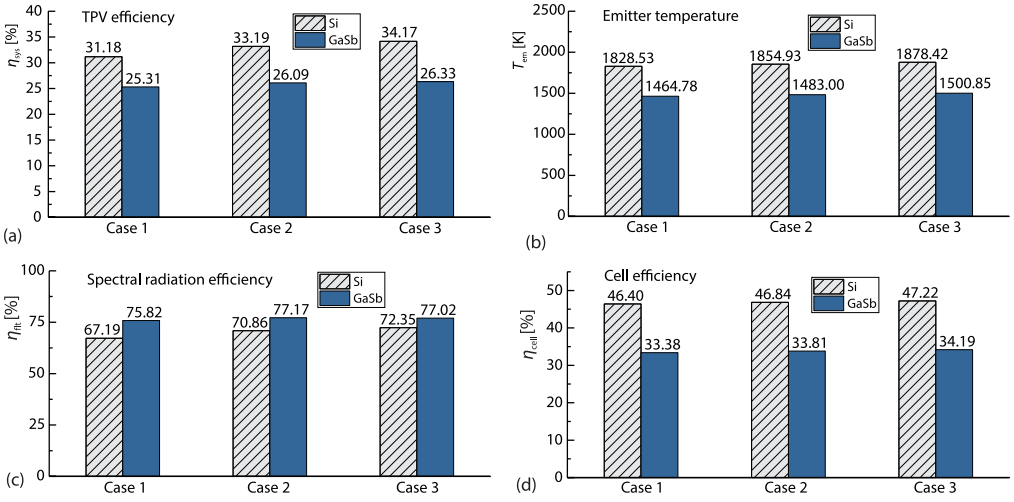

Figure 3. Effect of PV cell on system; (a) TPV efficiency, (b) emitter temperature, (c) spectral radiation efficiency, and (d) cell efficiency

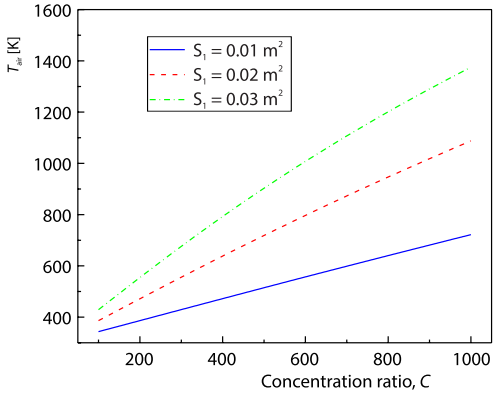

Figure 4. Effect of concentration ratio on preheated air temperature for different absorber areas

Effect of concentrate ratio

In this section, the influence of solar concentration ratio is discussed. Figure 4 shows the effect of the concentration ratio on the air preheating temperature Tair under basic cases (α = 0.9, ε_a = 0.2, E_c = 0.8, S_2 = 0.4 m^2) with different absorber areas S_1. It can be seen from fig. 4 that when S_1 is 0.01 m^2, the air temperature increases linearly with the concentration ratio. Due to the smaller S_1 area, its increase rate is lower than that of the other two cases. When S_1 is 0.03 m^2, the increase rate of air temperature gradually decreases with the concentration ratio. It should be noted that when C = 1000, T_{air}

of three cases are 722 K, 1088 K, and 1375 K, respectively. Thus, it indicates that when S_1 is 0.01 m^2 and 0.03 m^2, T_{air} is too low and too high, respectively. Considering that the concentration ratio of the current technology is generally below 1000, the S_1 of 0.02 m^2 is more suitable for the current technical conditions.

Furthermore, fig. 5(a) shows that when the absorber area S_1 is 0.02 m^2 and 0.03 m^2, with the continuous increase of the concentration ratio, the output power of the PV cell increases almost linearly, which increases by 7.15 kW and 9.91 kW, and the power density increased by 17.9 kW/m^2 and 24.8 kW/m^2, respectively. At the same time, the electrical efficiency of TPV system increased by 7.5 and 5.7 percent points, respectively. The increase of the concentration ratio causes the gradual increase of the emitter temperature, which improves the efficiency η_{cell} of the PV cell, resulting in a higher TPV system efficiency. It can be seen from fig. 5(a) that when C is greater than 500, the increasing trend of TPV system efficiency slows down. This is because P_{sol_in} increases greatly with the concentration ratio C. At the same time, as shown in fig. 5(b), the increase trend of η_{cell} *vs.* C is reduced, which also directly affects the system efficiency trend *vs*. C as in fig. 5(a). It can be seen that when S_1 is 0.02 m^2 and the concentration ratio is 500, the growth rates of the η_{sys} and η_{cell} begin to decrease significantly, when the area is 0.03 m^2, and the concentration ratio is 400, this trend also began to appear. Therefore, it does not make sense to select an excessively large emitter area and concentration ratio. In addition, it is worth noting that when designing the concentration ratio and the absorber area in practical engineering, attention should also be paid to the upper limit of the air preheating temperature, otherwise the pipe-line will be damaged by the working fluid [39]. Besides, some safety hazards during the combustion process may also arise. To sum up, the concentrating ratio suitable for this system can be selected between 400 and 500, and the absorber area can be selected as 0.02 m^2.

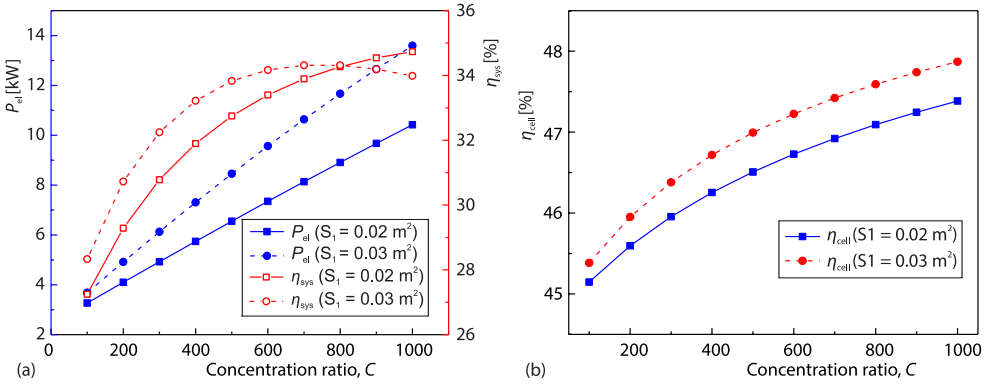

Figure 5. Effect of the concentration ratio on the power generation performance under different absorber areas; (a) PV cell output power and system efficiency and (b) PV cell efficiency

Effect of solar absorber coefficients

Furthermore, the effect of the absorptance, α, and heat transfer coefficient, E_c, of the solar absorber on the system performance is investigated. The basic case is set as C = 500, S_1 = 0.02 m^2, S_2 = 0.4 m^2. It can be seen from fig. 6(a) that when the absorption rate, α, changes from 0.6-0.9, the air preheating temperature increases from 583.8-719.2 K (a variation of about 130 K), and the system efficiency increases from 26-32.8%, showing an obvious trend. As can

be seen from fig. 6(b), when α is set to 0.75, the T_{air} increases from 648.7-653.6 K (a variation of about 5 K) with the increase of E_c from 0.6-1, while the system efficiency increases from 29.2% to 29.5%, showing a slight change. Therefore, it can be concluded that for solar absorber, it is more significant to improve the absorptance, α, than to optimize the heat exchanger efficiency E_c. In recent years, selective coating absorbing materials can achieve a high absorptance more than 90% [19], which is a potential research direction in the future.

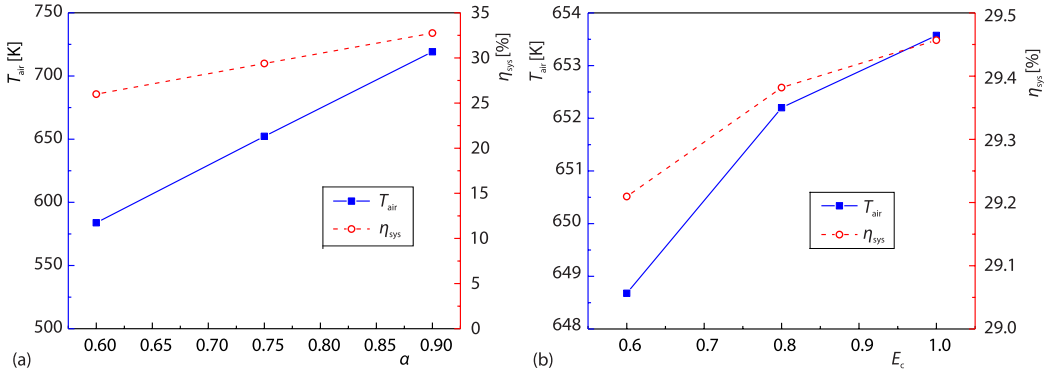

Figure 6. Effects of (a) radiation absorptance and (b) heat transfer coefficient of solar absorber on system performance

Effect of emitter area

The emitter area S_2 determines the amount of thermal radiation from the combustion chamber, which directly affects the performance such as the output power and system efficiency. Therefore, the determination of the emitter area is also particularly important. Figure 7 reflects the effect of emitter area (C = 500, S_1 = 0.02 m^2, S_2 = 0.4 m^2). It can be seen from fig. 7(a) that as the S_2 increases from 0.05-0.45 m^2, the output power increases from 5.15-6.6 kW. This is mainly because the radiative power is proportional to the emitter area. In addition, it can also be seen that the emitter temperature gradually decreases from 2264-1777 K, which is due to the thermal-balance result after the area increases. Due to the decrease in temperature, the output power increases faster first and then slower. On the other hand, fig. 7(b) also shows that the system efficiency η_{sys} increases from the initial 25.7-33% with the the emitter area, and showing a trend of increase fast first and slow then, which is consistent

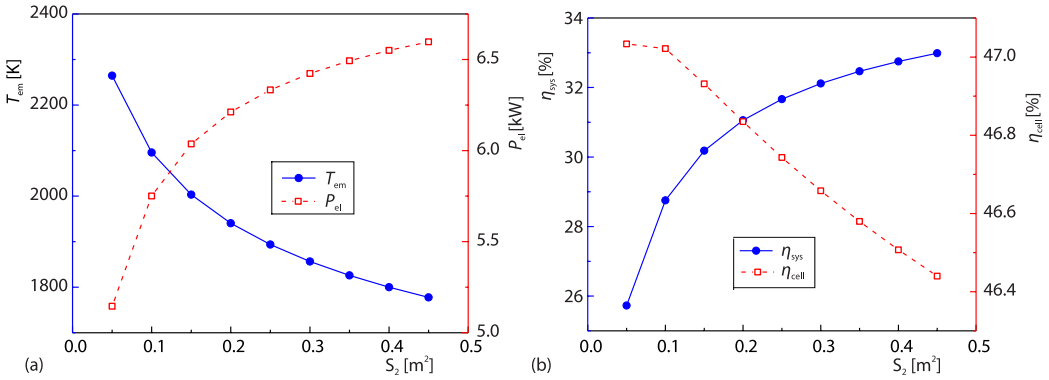

Figure 7. Effect of emitter areas on solar-fuel assisted TPV system; (a) output power and emitter temperature and (b) system efficiency and cell efficiency

with the power results in fig. 7(a). This is mainly due to the dual effects of emitter area and temperature. In addition, the cell efficiency decreases from 47-46.4% with emitter area, which is mainly due to the decrease in emitter temperature. Therefore, in practical applications, it is not possible to blindly increase the emitter area to increase the output power and system efficiency of the PV cell. Sometimes, a small-area emitter under a high temperature environment may bring higher energy conversion efficiency than a large-area emitter in a low temperature environment.

Energy-saving effect with solar-fuel assisted design

This section analyzes the energy-saving effect of the solar-fuel assisted system, the basic case is selected with $S_1 = 0.02$ and $S_2 = 0.4$ m^2. As shown in fig. 8(a), as the ratio of solar energy to fuel oil input, r, increases from 0-2, the system efficiency η_{sys} increases from 24.4-34.7% with an increase of about 10 percentage points. This indicates that with the complementary of solar energy, the energy conversion efficiency of the system is improved, which is mainly because the introduction of solar energy increases the air preheating temperature, T_{air}, which increases the combustion temperature, T_g, thereby increasing the emitter temperature, T_{em}, and improving the TPV system efficiency. It can also be seen that when the ratio r is greater than 1, the increase rate of the system efficiency slows down. Figure 8(b) shows the energy-saving characteristics of solar-fuel assisted TPV system. When the input ratio r increases from 0.2-2, the energy-saving rate θ_{egy} of the system increases from 10.45-29.76%, which is the result of the increase in system efficiency. At the same time, the fuel-saving rate θ_{fuel} of the system increases from 25.4-76.6%, which results from the simultaneous effect of the system efficiency increase and the solar energy complementary. This fully indicates the advantages of introducing solar energy into fuel-driven TPV. However, if too much solar radiation is introduced to preheat the air, it will also bring higher costs and safety hazards to the system, so the ratio of solar energy to fuel input can be controlled at about 1.

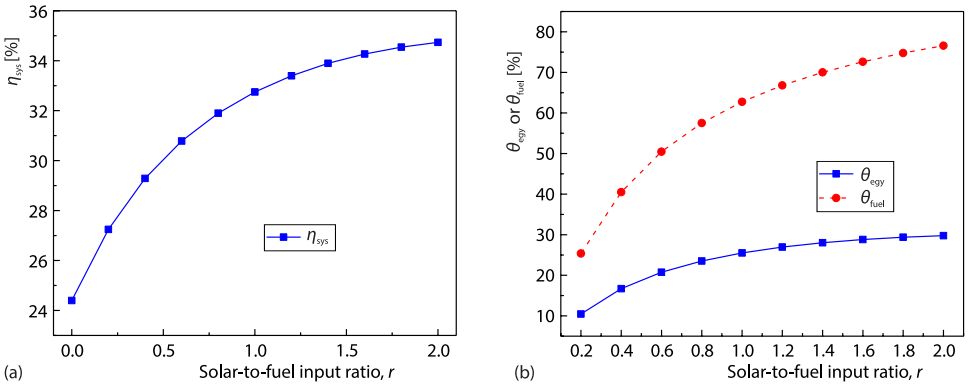

Figure 8. Effect of solar-to-fuel input ratio on the system performance; (a) system efficiency and (b) energy and fuel savings characteristics

Annual performance results

The solar radiation calculation model in [40] is used in this study. The Hangzhou City of China is taken as an example (Longitude: 120.1°, Latitude: 30.2°). The satellite measurements show that the global tilted irradiation is 1362.5 kWh/m^2 every year and the average air temperature is 17.6 °C. The efficiency and energy saving performance in a typical day of each month

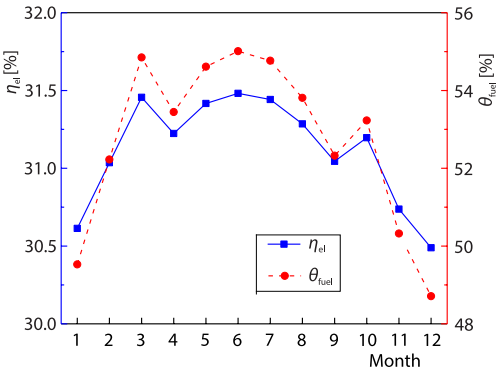

Figure 9. System electrical efficiency and fuel saving rate in a typical day of each month

are calculated. Here, the basic case (C = 500, S_1 = 0.02, S_2 = 0.4 m^2, P_{in} = 10 kW) is selected. Figure 9 shows the power generation efficiency η_{el} and fuel saving rate θ_{fuel} of system for typical days in each month. It can be seen that, the η_{el} of system is around 30-31%, which is higher in summer than in winter. Further, the system overall performance within one year is calculated. The results show that if the non-assisted system is used, the annual fuel consumption is about 50000 kWh, and the annual fuel saving of the assisted system achieves 52.93%. The annual electrical efficiency of the system reaches 31.14%, which is about 6% points higher than the non-assisted system (24.40%).

Conclusions

This study innovatively proposes a design concept of solar-fuel assisted TPV system and analyzes the parameters such as concentration ratio, absorber area, emitter area, solar-to-fuel input ratio on the system performance. This study provides a reference for the design of STPV and fuel-driven TPV systems, and its main conclusions are as follows.

- The system performance is better when Si cell is used, the electrical efficiency is around 6-8 percentage points higher than that of GaSb cell. This is because the cut-off wavelength of the selective filter matched to the Si cell is smaller than that of GaSb cell, so the emitter temperature after thermal balance is higher. In addition, since Si cell are more affordable, it has practical value in application.
- With the continuous increase of the concentration ratio, the output power density of the TPV cell can increase by nearly 25 kW/m^2, and the electrical efficiency of the TPV system can increase by nearly 10%. At the same time, the increase rate of PV cell efficiency gradually decreases. Considering the economic cost and system safety, the concentrating ratio suitable for solar-fuel assisted TPV system can be selected to be around 500. The solar absorber area should not be too large to ensure a reasonable solar-to-fuel input ratio.
- When the absorptance, α, of the solar absorber increases from 0.6-0.9, the system efficiency can be increase by about 7 percentage points, and the increase effect is more obvious. Compared with the heat exchanger efficiency, E_c, it is more significant to improve the absorptance of solar absorber in system optimization.
- The emitter area of TPV is the main factor affecting the output power of PV cells and the system efficiency. At the same time, as the emitter area increases, the emitter temperature decreases based on thermal balance, so the increasing rate of the output power decreases gradually. Therefore, in the solar-fuel assisted TPV system, the selection of emitter area is not as large as possible.
- The solar-fuel assisted TPV system has a significant energy-saving effect. When the solar-to-fuel input ratio increases from 0.2-2, the system energy-saving ratio increases from 10.45-29.76%. At the same time, the system fuel-saving ratio increases from 25.4-76.6%. This results from the simultaneous effect of system efficiency increase and solar-fuel complementary. Considering that the introduction of too much solar radiation preheat the air will also bring safety hazards to the system, so the ratio of solar energy to fuel input can be controlled at about 1.

In the future, a small-scale experimental set-up for solar-fuel assisted system should be built to investigate the actual operational performance. In addition, narrow-band photonic crystal emitters and filters adapted to Si cells should be designed to enhance the performance of the TPV system.

Acknowledgment

This work was supported by National Postdoctoral Program for Innovative Talents of China (BX2021254), China Postdoctoral Science Foundation (2021M702793) and Open Project of Key Laboratory of Solar Energy Utilization & Energy Saving Technology of Zhejiang Province (ZJS-OP-2020-14).

Nomenclature

C – concentration ratio of solar collector
C_p – specific heat, [Jkg^{-}1K^{-1}]
FF – fill factor
G – solar radiation intensity, [Wm^2]
h – surface heat transfer coefficient, [Wm^{-2}K^{-1}] or enthalpy, [kJkg^{-1}]
J_{sc} – short-circuit current, [A]
LHV – lower heating value, [kJkg^{-1}]
$\dot{m}$ – mass-flow rate, [kgs^{-1}]
P – power, [kW]
S – surface area, [m^2]
T – temperature, [K]
V_{oc} – open-circuit voltage, [V]

Greek symbols

α – absorptivity
ε – emissivity
η – efficiency
λ – wavelength, [m]
ρ – reflectivity

Subscripts

ab – absorber
af – adiabatic flame temperature
cp – combustion product
el – electrical energy
em – emitter
f – flame
flt – filter
g – flue gas
out – outlet
sys – system
sol – solar radiation
w – wall
0 – ambient
1 – tube receiver of solar collector
2 – emitter

References

[1] Pazheri, F., *et al*., A Review on Global Renewable Electricity Scenario, *Renewable and Sustainable Energy Reviews*, *31* (2014), Mar., pp. 835-845
[2] Su, S., *et al*., Solar Energy Utilization Patterns for Different District Typologies Using Multi-Objective Optimization: A Comparative Study in China, *Solar Energy*, *155* (2017), Oct., pp. 246-258
[3] Bitnar, B., *et al*., Thermophotovoltaics on the Move to Applications, *Applied Energy*, *105* (2013), May, pp. 430-438
[4] Bauer, T., Thermophotovoltaics: *Basic Principles and Critical Aspects of System Design*, Springer Science and Business Media, Heidelberg, Germany, 2011
[5] Ferrari, C., *et al*., The Critical Role of Emitter Size in Thermo-Photovoltaic Generators, *Solar Energy Materials and Solar Cells*, *113* (2013), June, pp. 20-25
[6] Shan, S., *et al*., Effect Evaluation of Micro/Nanostructured Materials on the Performance of Solar ThermoPhotovoltaic System: An Analysis Based on Measurement Data, *Solar Energy*, *231* (2022), Jan., pp. 1037-1047
[7] Shan, S., *et al*., Comparison between Spectrum-Split Conversion and Thermophotovoltaic for Solar Energy Utilization: Thermodynamic Limitation and Parametric Analysis, *Energy Conversion and Management*, *255* (2022), 115331
[8] Rephaeli, E., *et al*., Absorber and Emitter for Solar Thermo-Photovoltaic Systems to Achieve Efficiency Exceeding the Shockley-Queisser Limit, *Optics Express*, *17* (2009), 17, pp. 15145-15159
[9] Shan, S., *et al*., Spectral Emittance Measurements of Micro/Nanostructures in Energy Conversion: A Review, *Frontiers in Energy*, *14* (2020), 3, pp. 482-509

[10] Nam, Y., *et al*., Solar Thermophotovoltaic Energy Conversion Systems with 2-D Tantalum Photonic Crystal Absorbers and Emitters, *Solar Energy Materials and Solar Cells*, *122* (2014), Mar., pp. 287-296
[11] Ni, Q., *et al.*, Theoretical Analysis of Solar Thermophotovoltaic Energy Conversion with Selective Metafilm and Cavity Reflector, *Solar Energy*, *191* (2019), Oct., pp. 623-628
[12] Chen, M., *et al*., Performance Analysis of Solar Thermophotovoltaic System with Selective Absorber/Emitter, *Journal of Quantitative Spectroscopy and Radiative Transfer*, *253* (2020), 107163
[13] Lenert, A., *et al*., A Nanophotonic Solar Thermophotovoltaic Device, *Nature Nanotechnology*, *9* (2014), 2, pp. 126-130
[14] Ungaro, C., *et al*., Solar Thermophotovoltaic System Using Nanostructures, *Optics Express*, *23* (2015), 19, pp. A1149-A1156
[15] Bhatt, R., *et al*., Design and Validation of a High-Efficiency Planar Solar Thermophotovoltaic System Using a Spectrally Selective Emitter, *Optics Express*, *28* (2020), 15, pp. 21869-21890
[16] LaPotin, A., *et al*., Thermophotovoltaic Efficiency of 40%, *Nature*, *604* (2022), 7905, pp. 287-291
[17] Seyf, H., *et al*., Thermophotovoltaics: A Potential Pathway to High Efficiency Concentrated Solar Power, *Energy and Environmental Science*, *9* (2016), 8, pp. 2654-2665
[18] Chen, B., *et al*., An Effective Design of Thermophotovoltaic Metamaterial Emitter for Medium-Temperature Solar Energy Storage Utilization, *Solar Energy*, *231* (2022), Jan., pp. 194-202
[19] Chen, B., *et al.*, A Novel Molten Salt Energy Storage-Solar Thermophotovoltaic Integrated System with Mid-Temperature Metamaterial Spectrum Reshaping, *Solar Energy Materials and Solar Cells*, *243* (2022), 111799
[20] Rovira, A., *et al*., Comparison of Different Technologies for Integrated Solar Combined Cycles: Analysis of Concentrating Technology and Solar Integration, *Energies*, *11* (2018), 5, 1064
[21] Li, Y., *et al*., Optimization Study for Integrated Solar Combined Cycle System, *Journal of Engineering Thermophysics*, *35* (2014), 12, pp. 2348-2352
[22] Li, J., *et al*., A Potential Heat Source for the Micro-Thermophotovoltaic (TPV) System, *Chemical Engineering Science*, *64* (2009), 14, pp. 3282-3289
[23] Bani, S., *et al.*, Micro Combustion in a Porous Media for Thermophotovoltaic Power Generation, *Applied Thermal Engineering*, *129* (2018), Jan., pp. 596-605
[24] Mustafa, K., *et al*., Comparative Assessment of a Porous Burner Using Vegetable Cooking Oil-Kerosene Fuel Blends for Thermoelectric and Thermophotovoltaic Power Generation, *Fuel*, *180* (2016), Sept., pp. 137-147
[25] Mustafa, K., *et al.*, Experimental Analysis of a Porous Burner Operating on Kerosene-Vegetable Cooking Oil Blends for Thermophotovoltaic Power Generation, Energy Conversion and Management, *96* (2015), May, pp. 544-560
[26] Kang, X., *et al.*, Experimental Demonstration of a Novel Approach to Increase Power Conversion Potential of a Hydrocarbon Fuelled, Portable, Thermophotovoltaic System, *Energy Conversion and Management*, *133* (2017), Feb., pp. 127-137
[27] Peng, Q., *et al*., Investigation on Premixed H_2/C_3H_8/Air Combustion in Porous Medium Combustor for the Micro Thermophotovoltaic Application, *Applied Energy*, *260* (2020), 114352
[28] Shan, S., *et al*., An Innovative Integrated System Concept between Oxy-Fuel Thermo-Photovoltaic Device and a Brayton-Rankine Combined Cycle and Its Preliminary Thermodynamic Analysis, *Energy Conversion and Management*, *180* (2019), Jan., pp. 1139-1152
[29] Shan, S., *et al*., New Oxy-Fuel Cascade Thermo-Photovoltaic Energy Conversion System: Effect of Cascade Design and Oxygen Ratio, *Energy Conversion and Management*, *196* (2019), Sept., pp. 1208-1221
[30] Wei, J., *et al*., Investigation on the H_2 Fueled Combustion with CH_4 and $C3H_8$ Blending in a Micro Tube with/without Fins, *Fuel*, *328* (2022), 125314
[31] Gupta, M., *et al*., Numerical Modelling and Performance Enhancement of Micro Combustor Powered Thermophotovoltaic Systems Using High Contrast Gratings, *Applied Thermal Engineering*, *215* (2022), 118935
[32] Meng, C., *et al*., Selective Emitter with Core-Shell Nanosphere Structure for Thermophotovoltaic Systems, *Energy*, *239* (2022), 121884
[33] Ferrari, C., *et al*., Thermophotovoltaic Energy Conversion: Analytical Aspects, Prototypes and Experiences, *Applied Energy*, *113* (2014), Jan., pp. 1717-1730
[34] Stephen, R., *An Introduction Combustion: Concepts and Applications*, McGrw-Hill Companies Inc., New York, USA, 2000
[35] Rong, L., *et al.*, *Principle of Power Station Boiler* (in Chinese), Zhejiang University Press, Hangzhou, China, 1999

[36] Shan, S., *et al.*, New Pressurized WSGG Model and the Effect of Pressure on the Radiation Heat Transfer of H_2O/CO_2 Gas Mixtures, *International Journal of Heat and Mass Transfer*, *121* (2018), June, pp. 999-1010
[37] Zhang, Y., *et al.*, *Theory and Calculation of Heat Transfer in Furnace*, Elsevier, Amsterdam, The Netherlands, 2016
[38] Shoaei, E., *et al*., Performance Assessment of Thermophotovoltaic Application in Steel Industry, *Solar Energy Materials and Solar Cells*, *157* (2016), Dec., pp. 55-64
[39] Quero, M., *et al*., Solugas-Operation Experience of the First Solar Hybrid Gas Turbine System at MW Scale, *Energy Procedia*, *49* (2014), Dec., pp. 1820-1830
[40] Gholamalizadeh, E., Chung, J., Exergy Analysis of a Pilot Parabolic Solar Dish-Stirling System, *Entropy*, *19* (2017), 509

Paper submitted: September 10, 2022
Paper revised: October 15, 2022
Paper accepted: October 21, 2022